Cement & Concrete Composites 33 (2011) 276–285

Contents lists available at ScienceDirect

Cement & Concrete Composites

journal homepage: www.elsevier.com/locate/cemconcomp

Resistance of concrete mixtures to cyclic sulfuric acid exposure and mixed sulfates: Effect of the type of aggregate

F. Girardi, R. Di Maggio *

Department of Materials Engineering and Industrial Technologies, University of Trento, Via Mesiano 77, 38100 Trento, Italy

ARTICLE INFO

Article history:
Received 5 October 2009
Received in revised form 20 October 2010
Accepted 22 October 2010
Available online 27 October 2010

Keywords:
Ammonium sulfate attack
Sulfuric acid attack
SEM
Gypsum
Dolomitic limestone
Natural aggregate

ABSTRACT

The behavior of different concrete mixtures was examined in relation to their exposure both to different metal sulfate solutions and alternately to metal sulfates and sulfuric acid, recording the expansion and mass loss of the test specimens for about three years. The test method adopted in this study can be considered a model of accelerated deterioration, more closely resembling the situation in sewer pipes than in sulfate-bearing soil. Three different cements – i.e. Portland limestone (PLC), blast furnace slag (BFC) and pozzolanic (PZC) cement (this last with silica fume, SF) – were used to prepare the concretes mixtures. Half of the samples were prepared using a ground dolomitic limestone and the other half with a natural aggregate. The greatest expansion and most severe damage were surprisingly recorded for the BFC and PZC + SF samples, in a two-stage process of deterioration. The degradation was particularly severe when the samples contained natural aggregate and under cyclic exposure to solutions of mixed sulfates and sulfuric acid. A continuous web of cracks within the cement paste and through the aggregate particles was seen on SEM. EDX analyses enabled us to establish gypsum nucleates in the cracks, causing expansion and aggregate detachment. Portland limestone cement is the best choice when a concrete is liable to attack by these different aggressive species, regardless of the type of aggregate used. For comparison, the same types of sample were exposed to attack by mixed sulfates alone.

1. Introduction

Concrete shows extensive degradation when exposed to sulfate-bearing solutions or polluted ground waters, as in wastewater and sewage facilities [1–5]. Concretes may deteriorate due to an inadequate mix design and the aggressive nature of certain environments warrants extra precautions to increase their durability [6].

The processes leading to corrosion in concrete sewer pipes are highly complex, still far from fully understood. As reported by several authors [7–16], hydrogen sulfide produced by anaerobic wastewater is converted into sulfuric acid by micro-organisms, such as *Thiobacillus thiooxidans*, and this acid reacts with the concrete [17]. First it attacks the calcium hydroxide, and the C–S–H too as soon as portlandite is no longer available, making the calcium hydroxide form gypsum and the calcium silicate hydrate (C–S–H) form both anhydrous gypsum and an incoherent mass of hydrated silicate. In a second step, calcium aluminate hydrate reacts with the sodium sulfate ions from the sulfuric acid, forming ettringite ($3CaO{\cdot}Al_2O_3{\cdot}3CaSO_4{\cdot}32H_2O$). It seems that the concrete would need to be formulated to resist both acid and sulfate attack.

An acid environment is thus one of the most harmful for concrete. According to the EN standard 206, aggressive environments are divided into exposure classes, depending on the severity of the attack. Sewer pipes come under exposure class XA3. The deterioration of concrete sewer pipes is a major problem if their service life is less than 30 years, so that damaged pipes need maintenance or even have to be replaced. There are currently no methods available for assessing the performance of hydraulic cements in acid- and sulfate-rich environments. In fact, the ASTM describes two test methods for assessing their performance in sulfate-rich environments (ASTM C452 and C1012), both of which have been criticized because they seem unable to predict field performance adequately. Among the several issues relating to these tests, it is worth noting that they are performed on mortars, not concretes, taking into account only the expansion due to ettringite formation. Acid attack is generally ignored, though it causes mass loss and may accelerate the deterioration process induced by sulfate exposure.

In a previous work, an accelerated test procedure was used to assess the effect of composition on the long-term durability and microstructure of a concrete cyclically exposed to solutions of sodium sulfate and sulfuric acid (pH = 2) [18]. This test method was used to obtain indications on the long-term performance of concretes containing Portland limestone cement (PLC), blast furnace slag cement (BFC), or sulfate-resistant pozzolanic cement,

* Corresponding author.
E-mail addresses: fabrizio.girardi@ing.unitn.it (F. Girardi), rosa.dimaggio@unitn.it (R.D. Maggio).

0958-9465/$ - see front matter © 2010 Elsevier Ltd. All rights reserved.
doi:10.1016/j.cemconcomp.2010.10.015

the latter two with and without silica fume (SF), at a constant water/cement ratio (*w/c* 0.39). The concrete prepared with pozzolanic cement and SF showed a generalized mass loss, but only negligible expansion even after lengthy periods of attack. Unfortunately, the method developed for testing resistance to both acid and sulfate only considers sodium sulfate attack, overlooking the fact that the actual field environment could include more aggressive compounds. The accelerated test could only approximate the actual conditions in sewer pipes, because different types of salts and metal sulfates can be found in wastewater.

Empirical and mechanistic models are found in literature for predicting the rate of sulfate attack and meantime the percentage of volumetric expansion of cement materials. It seems worth focusing on a test method for concretes involving a chemical attack, reproducing the field environment as nearly as possible. In the present study, we investigated the behavior of six different types of concrete exposed to a solution of mixed sulfate, including ammonium sulfate. The behavior of the same types of concrete was also observed after cyclic exposure to attack by sulfuric acid (pH = 2) and mixed sulfates.

What makes up the majority of a volume of concrete is the aggregate, which may or may not react with the chemicals to which it is exposed, depending on its acid or alkaline behavior. Such an interaction might modify the mechanisms and extent of degradation. Since the aggregates in concrete can vary from natural gravel or sand to crushed dolomitic limestone, depending on local availability, the effect of the type of aggregate under the same aggressive attack was also investigated.

2. Experimental

2.1. Materials

Six concrete pipes were prepared at the Eurobeton industrial plant in Salorno. The concretes were prepared in accordance with EN standard 206 for the XA3 class with a *w/c* ratio $\leqslant$0.45 and $R_{ck} \geqslant 45$ MPa. R_{ck} is the compressive characteristic resistance ($R_{ck} = R_{cm} - k\delta$, where $\delta = [\Sigma(R_{ci}-R_{cm})^2/(n-1)]^{1/2}$ and $k = 1.4$), the value for which there is a probability of 95% that each experimental strength result R_{ci} is higher than R_{ck}. The pipes were 30 cm in diameter and 200 cm long. Their minimum and maximum thicknesses were 57 and 100 mm (at the bottom). Their chemical composition and the concrete mix designs are detailed in Table 1. Two types of aggregate were used: the first was prepared by crushing a dolomitic limestone. The second consisted of natural gravel and sand. The characteristics of the aggregates are given in Table 2. For the sake of simplicity, the first type of aggregate was labeled as "limestone" and all the samples containing it as L-samples. Likewise, the second type of aggregate was labeled as "silicate" and all the samples containing it as S-samples.

To compare the chemical resistance of different cements, a PLC (CEM II/A-LL 42.5 R), a BFC (CEM III/A 42.5) and a pozzolanic one (CEM IV/A [P] 42.5) with low aluminate content were considered. As detailed in Table 1, the pozzolanic samples also contained silica fume (SF) and an acrylic superplasticizer admixture.

The pipes were removed from the mould after 1 day, then matured in the open air and sprinkled with water when the relative humidity was below 80%. The temperature was about 27 °C. After 30 days, two sets of cylindrical samples 30 mm in diameter and 140 mm high were cored directly from the pipes. The two sets were used for each of the two chemical tests, as described in the following paragraph.

2.2. Chemical test procedures

The chemical resistance of the concrete samples to the following types of attack was investigated at 20 ± 2 °C:

(a) a cyclic immersion in the solution of mixed sulfates (described in Table 3), replenished monthly, combined with one 6-h immersion a month in 2 l of sulfuric acid solution with a pH 2, representing an exposure closer to those expected in sewer pipes;
(b) continuous immersion in 2 l of mixed sulfate solution (described in Table 3), replenished monthly, representing the an exposure closer to those expected for underground concrete structures.

Every month, the length and weight of each sample were measured. Their weight was recorded, after drying the samples with a cloth, using a technical balance with a sensitivity of 0.001 g. Their length was measured with a digital comparator with a precision of 0.001 mm. pH values of the attack solution during the samples storage were measured by a pH-meter (pH 315i WTW), with a sensitivity of ±0.01.

After about 33,000 h of attack, microstructural analyses were performed using a SEM (Philips LX30) equipped with means for energy-dispersive X-ray analysis (EDX) and the phenolphthalein method (EN 9944).

XRD (40 kV–22.5 mA) analyses were performed with an Imaging Plate diffractometer (Italstructure) in pure reflection geometry, with a Cu Kα anode, a Si multilayer monochromator on the incident beam and a Ni filter on the diffracted beam; the I.P. acquisition system was a Perkin–Elmer Pico Cyclone scanner. A full-

Table 1
Concrete mixtures.

Aggregate	Limestone (dolomite)			Silicate (natural gravel and sand)		
Mixture	PLC-L	BFC-L	PZC-L + SF	PLC-S	BFC-S	PZC-S + SF
Fine 0/2 (mm) (kg/m^3)	722	722	720	460	460	460
Fine 0/4 (mm) (kg/m^3)	412	412	410	460	460	460
Coarse 3/8 (mm) (kg/m^3)	621	621	620	400	400	400
Coarse 8/15 (mm) (kg/m^3)	205	205	205	680	680	680
Cement designation (EN 197)	CEM II/A-LL	CEM III/A	CEM IV/A	CEM II/A-LL	CEM III/A	CEM IV/A
Cement (kg/m^3)	355	355	340	400	400	400
Silica fume (Meyco, MS610) (kg/m^3)	–	–	30	–	–	30
Acrylic superplasticizer (Glenium) (kg/m^3)	–		2.8	–	–	2.8
Water (kg/m^3)	140	140	133	155	155	155
w/c	0.39	0.39	0.39	0.39	0.39	0.39
Mass volume density (kg/dm^3)	2.501	2.532	2.516	2.303	2.309	2.349

N.B.: Each mass was determined at industrial plant, with an error range of ±3%.

Table 2
Weight percentage (1% error) of aggregate phases determined by XRD.

		Quartz	Calcite	Feldspar	Dolomite
L-aggregate	Crushed dolomitic limestone	1	11	–	88
S-aggregate	Sand 0/2	52	12	36	–
	Sand 0/5	47	22	31	–
	Gravel 3/6	32	51	17	–
	Gravel 9/14	31	62	7	–

Table 3
Composition of sulfate solution.

	g/l
Na_2SO_4	30
$(NH_4)_2SO_4$	15
$MgSO_4$	10
NaCl	10
KH_2PO_4	3
Glucose	1

profile Rietveld refinement was done using material analysis using diffraction (MAUD) software.

3. Results

The XRD analyses performed on the two types of aggregate show that the first of the two is mainly dolomite, whereas the composition of the second varies depending on its size (Table 2). The two fractions of sand contained more quartz and feldspar, while the two fractions of gravel mainly consisted of calcite with a smaller amount of quartz and feldspar.

In order to bring about a severe attack, we used a solution of mixed sulfates alone, including ammonium sulfate, or alternately with a solution (pH = 2) of sulfuric acid. The mixed sulfate solution used in this study (Table 3) was slightly acid. Fig. 1a–d shows the typical trend of the pH of the aggressive solutions during the immersion of the samples. It is worth noting that the pH goes from lower to higher values in all cases except for the sulfuric acid solution in which the S-samples were immersed.

The results regarding the variation in mass and length of the L-samples are described first. Fig. 2a shows the percentage mass variation of the samples continuously exposed to mixed sulfate attack alone. The slope of the experimental curve is negative: the mass loss is due to the reaction of the acid solution with the alkaline substances in the concretes (cement paste and aggregate). Fig. 2b shows the percentage mass variation of the samples exposed to both mixed sulfate and acid attack. The specimens showed,

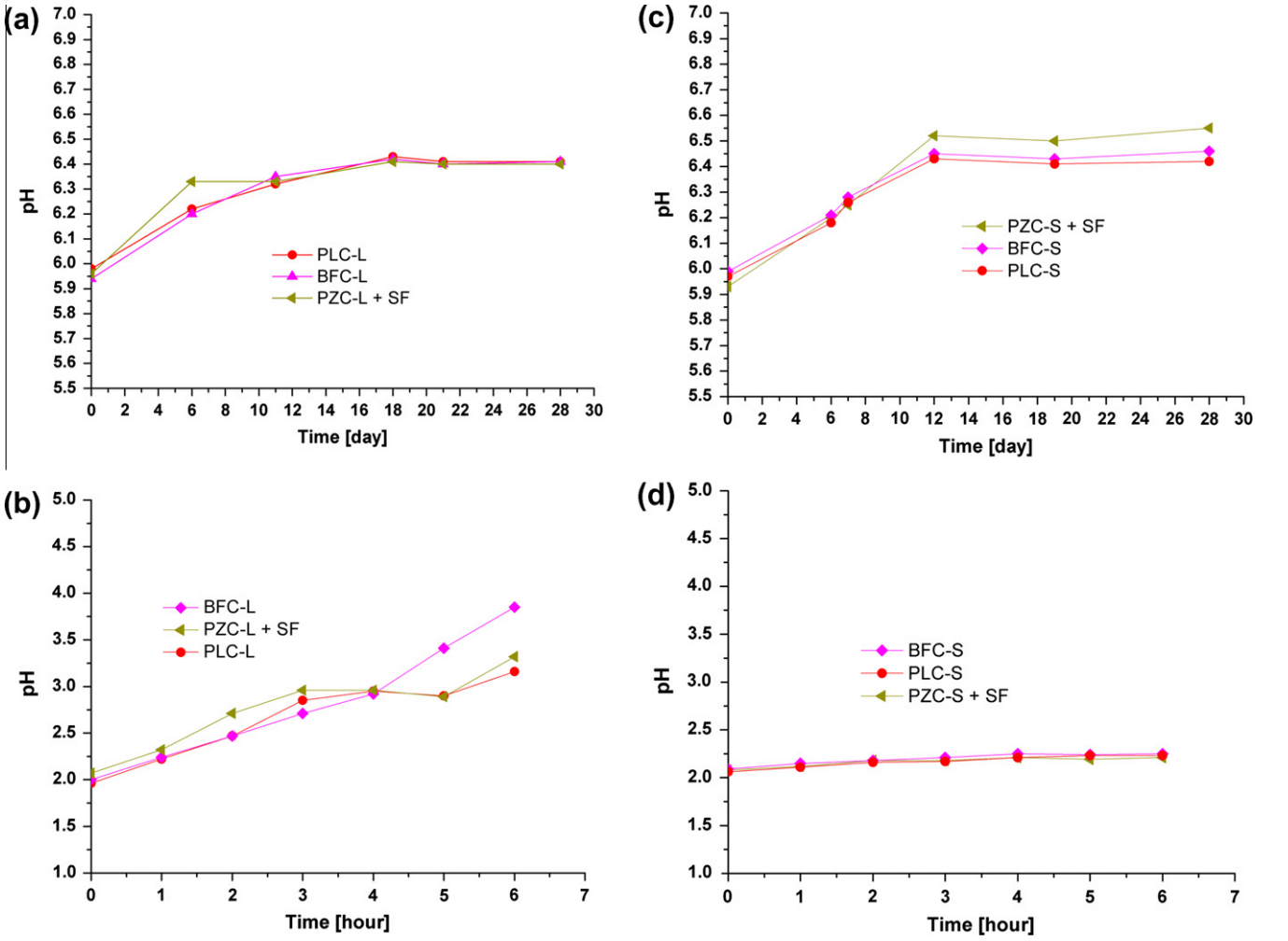

Fig. 1. pH of solutions of mixed sulfates (a) and sulfuric acid (b) *vs.* immersion time for L-samples; pH of solutions of mixed sulfates (c) and sulfuric acid (d) *vs.* immersion time for S-samples.

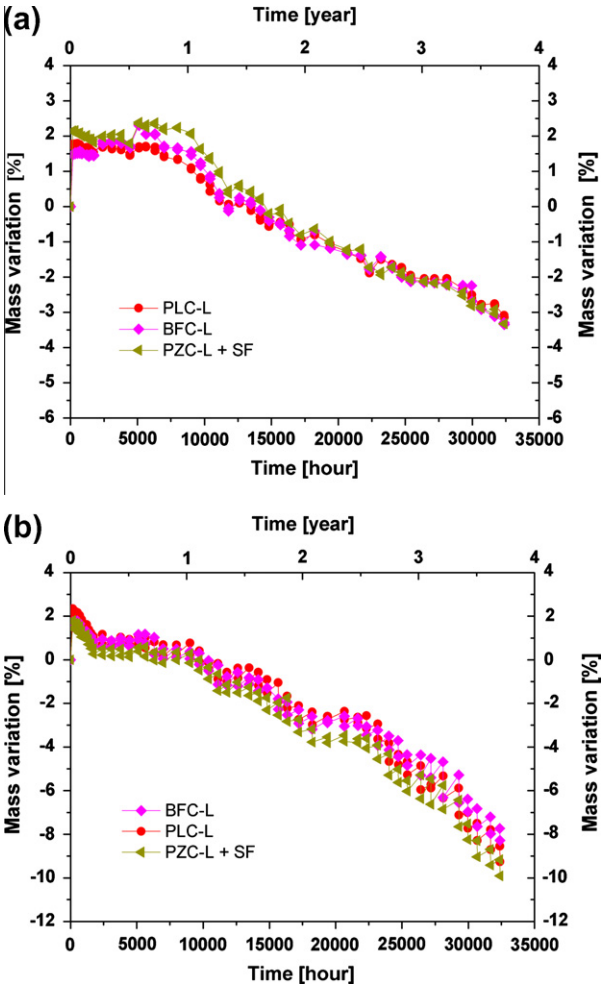

Fig. 2. Mass loss of L-samples in a mixed sulfate solution alone (a) and after cyclic mixed sulfate/acid attack (b) *vs.* time.

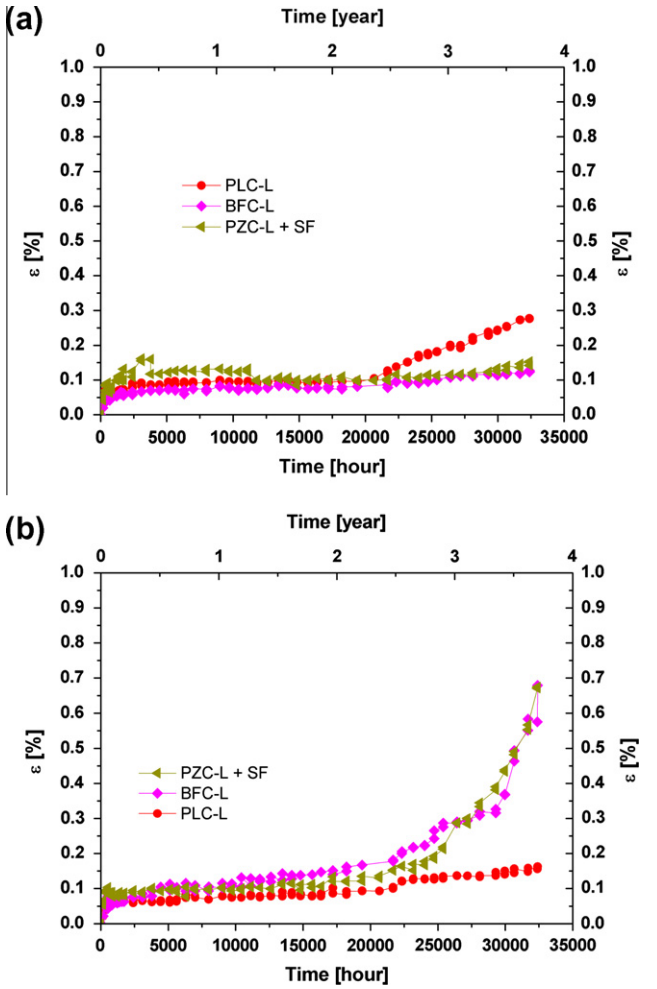

Fig. 3. Percentage strain of L-samples under mixed sulfate attack (a) and cyclic mixed sulfate/acid attack (b) *vs.* time.

similarly for all the samples, a constant decrease in mass, twice as severe as in the previous case due to the increased acidity of the attack.

Fig. 3a shows the expansions, in terms of the strain, of the specimens exposed to mixed sulfate attack alone and Fig. 3b those of the samples exposed to both mixed sulfate and acid attack. The expansion rate and total expansion were much lower in the first case than in the second. BFC-L and PZC-L + SF specimens showed a negligible expansion, whereas the expansion rate of PLC-L suddenly increased after a dormant period of about 20,000 h. Under the cyclic attack the PZC-L + SF and BFC-L expanded more than the PLC-L. It is worth noting that this last sample expanded even less than in the case of mixed sulfate attack alone. Moreover the dormant period reduced and the expansion occurred in two steps at lower and higher rate [19–21].

Microstructural analyses were performed after about 33,000 h of testing to monitor the deterioration of all the concretes involved in the cyclic tests. Immediately after cutting slices from samples, their core appeared alkaline with phenolphthalein indicator. Polished samples, taken from all five concretes, were examined by scanning electronic microscopy (SEM) using energy-dispersive X-ray analysis (EDX). Generally speaking, the concretes exhibit a more deteriorated surface zone and an interior zone where micro-cracks appear.

Actually, on SEM imaging (Fig. 4a), the surface of the PLC-L sample showed few small cracks. Fig. 4b is the X-ray map for sulfur on the same sample, with sulfur filling the voids and the cracks. The interior zone appears dense and quite unaffected by attack. SEM observations of the surface of BFC-L and PZC-L + SF samples reveal long cracks in the cement paste, extensive cracking around aggregates and through the paste, with occasional cracking through aggregate particles too. Figs. 5a and 6a show their cutting surfaces, respectively. The X-ray maps of Figs. 5b and 6b indicate that the largest and long cracks contain nothing but sulfur (and calcium). Fig. 7 shows the magnification of large crystals grown in a crack of the PZC-L + SF sample under about 33,000 h of acid/sulfate attack. EDX analysis, here not reported, confirmed the presence of calcium and sulfur in these crystals and an atomic ratio Ca/S comparable with that of gypsum. A general result, for all the samples, is that the X-ray map for magnesium indicates always that this ion is everywhere in cement paste and of course in aggregate, unless into the crystals filling the cracks.

The following results regard the variation in mass and length of the S-samples. Fig. 8a shows the percentage mass variation in the samples exposed to continuous mixed sulfate attack alone, while Fig. 8b shows the variation in the samples exposed to both mixed sulfate and acid attack. The specimens showed a marked mass loss after 33,000 h of attack, despite negligible changes in the pH of the mixed sulfate and sulfuric acid solutions. All three types of concrete pipe showed a similar behavior in terms of mass variation in the first few months of the test. Then the rate of mass loss became slower in the PLC-S and BFC-S.

Fig. 9a shows the expansion, in terms of the strain, of the specimens exposed to mixed sulfate attack alone and Fig. 9b the

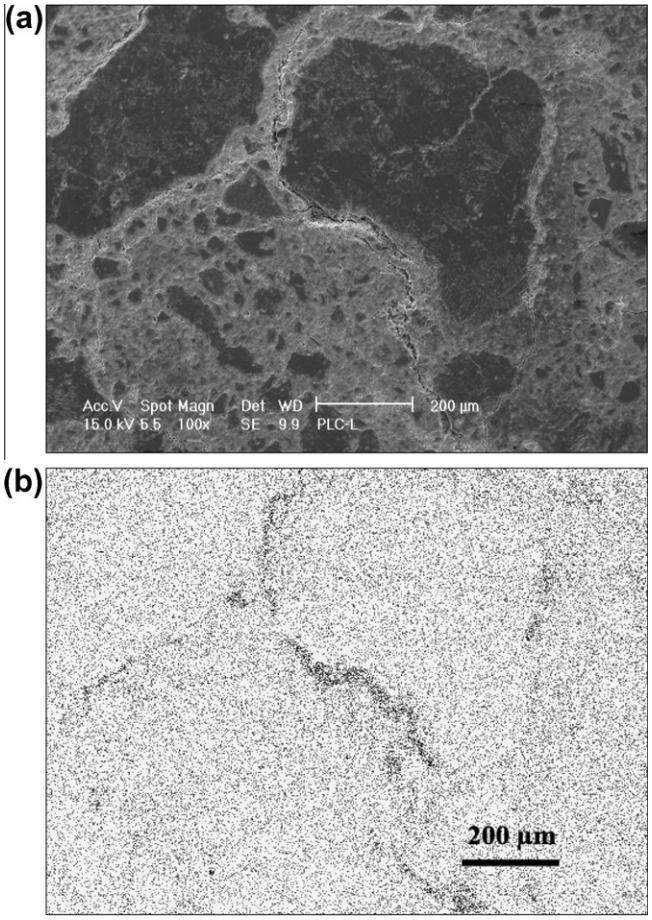

Fig. 4. SEM image (a) and X-ray maps for sulfur (dark) (b) on polished surface of PLC-L under cyclic sulfate/acid attack.

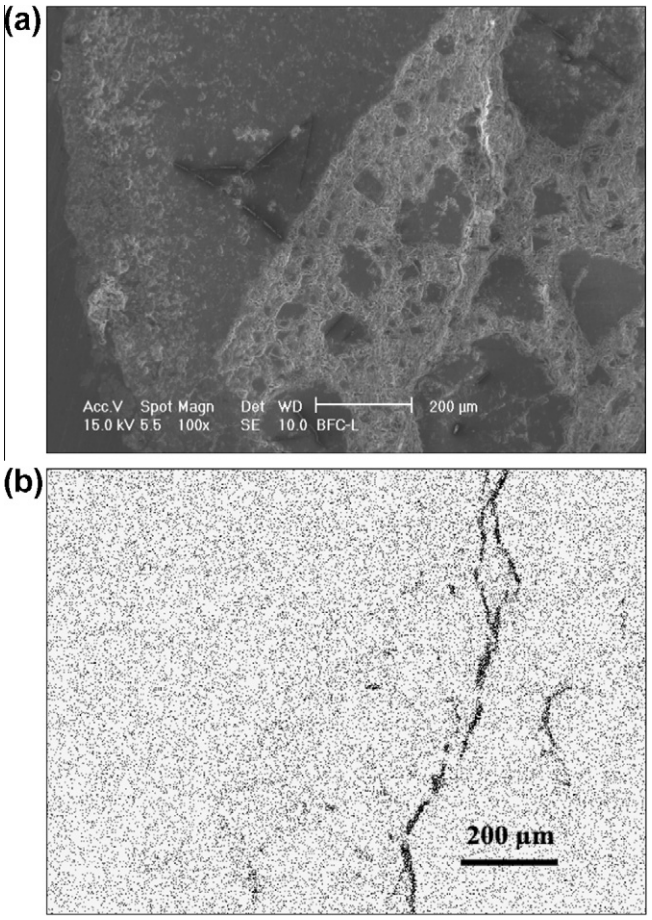

Fig. 5. SEM image (a) and X-ray maps for sulfur (dark) (b) on polished surface of BFC-L under cyclic sulfate/acid attack.

expansion of the samples exposed to both mixed sulfate and acid attack. The expansion rate was much slower in the former than in the latter and drastically increased with respect L-samples. It is worth noting that, for both types of attack, the PLC-S was the slowest to expand of the samples analysed. As in the L-samples, they expanded in two steps, but in this case the dormant period was very short (just 2500 h).

Microstructural alterations, resulting from the exposure to sulfate solutions during cyclic test, were analysed after 33,000 h by SEM and EDX. Immediately after cutting, the core of all the specimens appeared alkaline. Also for S-samples, the surface zone appears more deteriorated than the interior one and to a greater extent than L-samples. In Fig. 10a the surface of the PLC-S sample showed no remarkable signs of degradation and very few small cracks, which contain layered small crystals, only apparent under the strongest magnifications. Fig. 10b is the X-ray map for sulfur of the same sample, showing it filling cracks. Figs. 11a and 12a show the cutting surface of samples PZC-S + SF and BFC-S with an extensive cracking around and through both the aggregates and paste. In these samples large cracks are visible and filled of layered crystals, especially in the transition zone. Fig. 13 shows the magnification of these crystals in the BFC-S sample. Here again, EDX analysis confirmed the high sulfur content in these crystals and an atomic ratio Ca/S ratio comparable with that of gypsum. A general result, for all the samples, is that the X-ray map for magnesium indicates its presence in cement paste, especially on the cracks' edges of PLC-S samples, but not into the crystals filling the cracks.

4. Discussion

A reliable method for the accelerated testing of the resistance of concretes in harmful environments, as for example sewerage, is of growing interest. Evaluating resistance according to the ASTM C1012 standard (''Test Method for Length Changes of Hydraulic-Cement Mortars Exposed to a Sulfate Solution'', which indicates the exposure to sodium sulfate solution) takes too long, refers to mortars and overlooks the contribution of acid attack to the global degradation of concrete pipes. We used a test method that included immersion in a solution of mixed sulfates and a monthly sulfuric acid attack to better simulate the field environment. The resulting damage was assessed by measuring mass loss and expansion, in terms of strain. For comparison, a test was also performed using a solution of mixed sulfates alone.

The results of this study are very puzzling and suggest that the concretes' behavior depends on both the type of aggregate and the type of cement. Increasing the severity of chemical attack, supplementary cementing materials are not beneficial to improve resistance against deterioration [18,22].

The diffusion of sulfate ions into concretes from sulfate-containing solutions is coupled with portlandite or C–S–H dissolution, with a general loss of surface adhesion. As reported in the literature [23,24], the deterioration induced by ammonium sulfate conceals the other aggressive corrosion in concrete according to reactions (1) and (2):

$$Ca(OH)_{2(s)} + (NH_4)_2SO_{4(aq)} \rightarrow CaSO_4 \cdot 2H_2O_{(s)} + 2NH_{3(aq)} \quad (1)$$

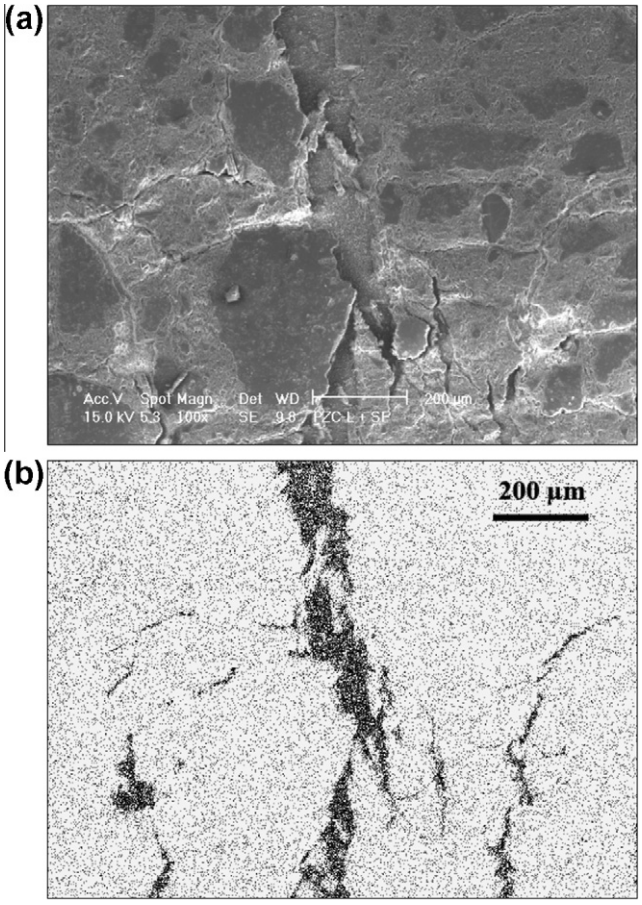

Fig. 6. SEM image (a) and X-ray maps for sulfur (dark) (b) on polished surface of PZC-L + SF under cyclic sulfate/acid attack.

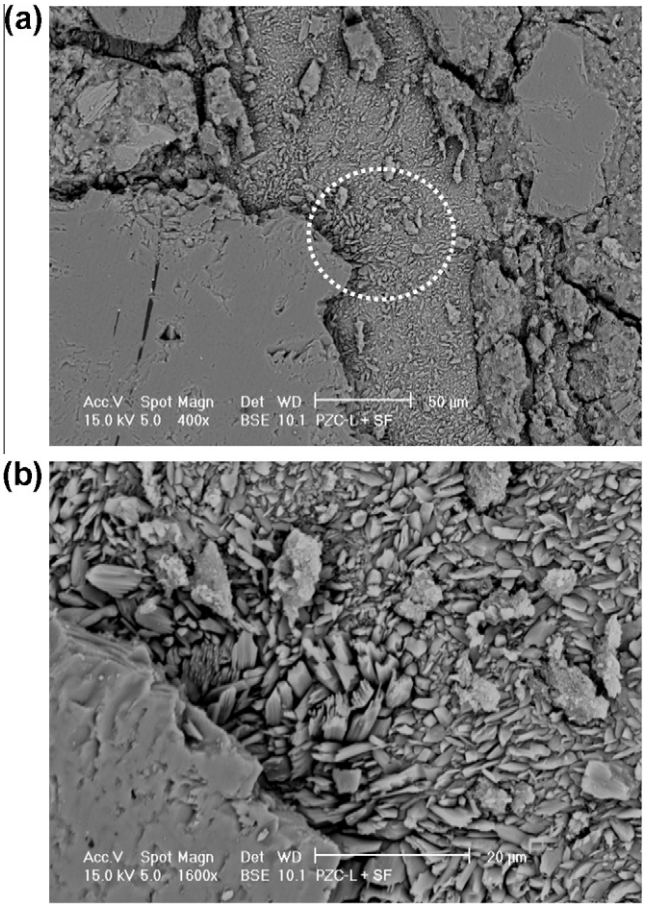

Fig. 7. SEM image of PZC-S + SF concrete (a). The dashed red circle outlines the area magnified in (b), containing layered crystals embedded in cracks in the transition zone.

$$C_3S_2H_{3(s)} + (NH_4)_2SO_{4(aq)} + H_2O \rightarrow CaSO_4 \cdot 2H_2O_{(s)} + C_2S_2H_{3(s)} + 2NH_{3(aq)} \quad (2)$$

This accounts for the small increase in pH of the mixed sulfates solution.

Under mixed sulfates attack alone, the L-samples lost more mass than the S-samples. Thus other reactions, such as those involving aggregates, have to take place to justify the mass loss. At this regard, it is worth noting that S-aggregate contains more calcium carbonate than L-aggregate, mainly dolomitic. In fact an unexpected beneficial effect of carbonate aggregate on resistance to conventional sulfate attack was found in literature, although the reaction are supposed involving a very small fraction of aggregate [25]. Actually, calcium carbonate was found to be available as source of calcium for gypsum (and ettringite) formation, reducing the extent of dissolution of portlandite and especially decalcification of C–S–H.

When exposed cyclically to sulfates and sulfuric acid, all the samples lost more mass than in the previous case: sulfuric acid enhances the effect of ammonium sulfate. In this case, L-samples surprisingly lost mass slower than the S-samples. Several reactions involving all the different chemical species in the mixed sulfate solution might take place, but overall the most important is the dissolution of portlandite [8], with the side effect of the nucleation of gypsum, the dissolution of dolomite, with the side effect of nucleation of $MgSO_4$ and the decalcification of C–S–H. Accordingly, pH of the attack solution of the L-samples increased significantly. Haga et al. reported that for a higher initial amount of $Ca(OH)_2$ it is larger the increase of pore volume, due to the dissolution of portlandite rather than C–S–H [26]. However, the negligible increase in the pH of the sulfuric acid solution during the immersion of the S-samples suggests that in this case the dissolution reactions remain somewhat limited and restricted to transition zone rather than over the whole surface. There are the surface spalling and detachment of aggregates due to the weakening of transition zone accounting for their greater mass loss. This is especially true for the PZC-S + SF and BFC-S concretes, which contain a low amount of free portlandite due to the pozzolanic reaction with SF and amorphous slag, respectively. When no more $Ca(OH)_2$ is readily available, both acid and mixed sulfates solution attack C–S–H, the main binding component of hardened cement paste, provoking mainly its decalcification in transition zone. In fact, their rate of mass loss was not constant and increased with time. Moreover as mentioned before S-aggregate actually contains much more calcite, which reacts more easily than dolomite with the acid and produces gypsum according to the reaction (3):

$$CaCO_{3(s)} + H_2SO_{4(aq)} + H_2O_{(l)} \rightarrow CaSO_4 \cdot 2H_2O_{(s)} + CO_{2(g)} \quad (3)$$

Dissolution leaves porosities and induces a faster diffusion of the aggressive species deeper inside the sample, even into the core of the specimens. As shown in the SEM images, the cement paste in these samples loses coherence with the aggregate particles, which eventually become detached. As a consequence, their surface is generally worn down.

The second destructive mechanism associated to diffusion of sulfate sulfate ions into concretes from sulfate-containing solutions is the formation of gypsum, where calcium hydroxide is

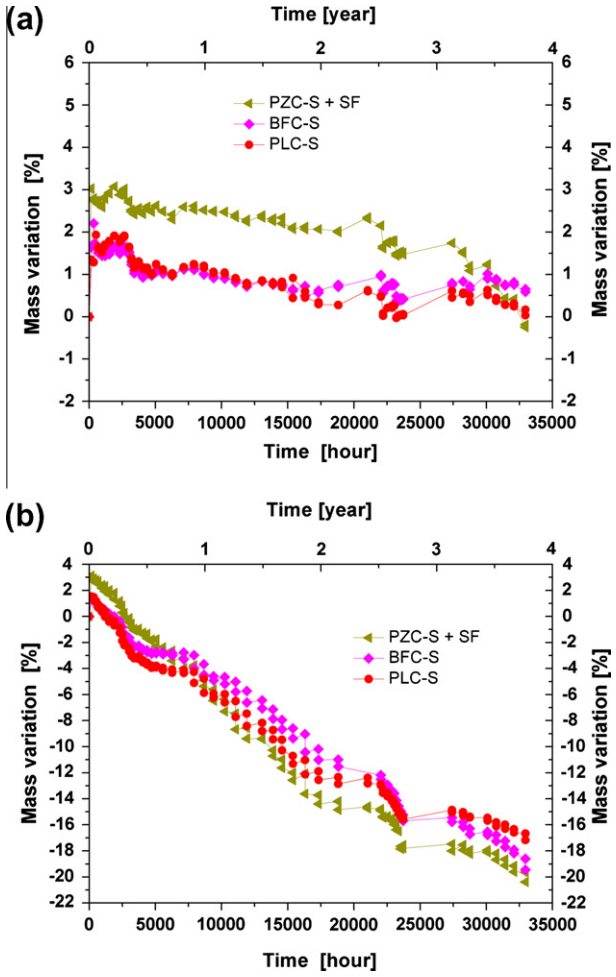

Fig. 8. Mass loss of the S-samples under mixed sulfate (a) and cyclic mixed sulfate/acid attack (b) *vs.* time.

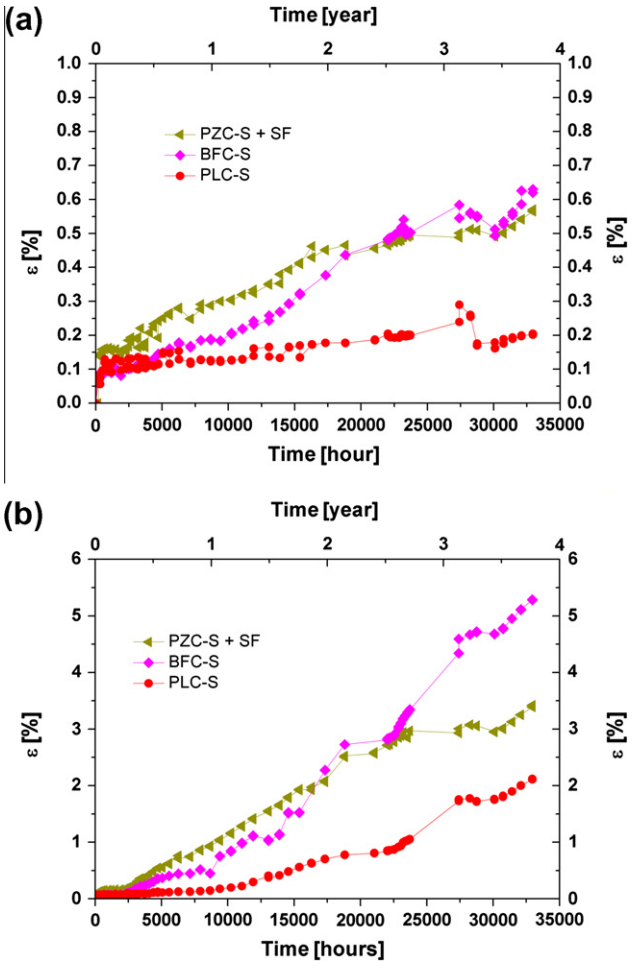

Fig. 9. Percentage strain of S-samples under mixed sulfate (a) and cyclic mixed sulfate/acid attack (b) *vs.* time.

reduced. This induces expansive forces and cracking. A general result of the present study was that columnar or layered crystals were grown in the cracks and visible through SEM observation: the greater the expansion the larger the cracks. Using EDX, the crystals embedded in the cracks revealed an atomic Ca/S ratio compatible with calcium sulfate and a negligible amount of different elements. Previous studies have already shown that gypsum forms instead of ettringite because of the high concentration of SO_4^{2-}, as in the present case [27–30]. Gypsum formation under sulfate attack is expansive [28–31], although ettringite may form afterwards and contribute to further expansion: the tinier the space, the higher the developed stresses and the expansion. Moreover, the growth of the crystals (as layers or columns) occurs inside the cracks. In the presence of magnesium ions the formation of brucite ($Mg(OH)_2$) can also occur by metathesis reaction between magnesium sulfate and portlandite or ammonium hydroxide. Moreover C–S–H can be replaced by M–S–H, bringing about more deterioration.

Expansion occurred in two steps in agreement with the results of previous studies on concretes stored in sodium sulfate solution [18–21]. When exposed only to mixed sulfates, the PLC-L and PLC-S showed a quite similar expansion. The BFC-L and PZC-L + SF samples expanded much less than the PZC-S + SF and BFC-S samples. Also the dormant period in the latter was much shorter than in the former. As discussed before, the calcium carbonate of the cement paste provides a source of calcium ions, which instead should be obtained by dissolution of portlandite and C–S–H. On the other hand, it induces more formation of gypsum and thus expansion [25].

When the concretes were exposed alternately to sulfuric acid and mixed sulfates, expansion was even more severe. The most important findings were that the PLC concrete, richer in portlandite and limestone, surprisingly expands the least of all, whatever the aggregate involved. At this regard, formation of magnesium hydroxide, less reactive and insoluble than portlandite, all over the whole surface had a protective though unpredictable effect [22,25]. Judging from the SEM findings, unlike the generalized dissolution seen in the L-specimens, the attack in the S-samples was concentrated on the transition zone beside the cement paste, producing localized narrow defects and micro-cracks around aggregates, in which gypsum nucleated during the induction period. As seen in the SEM images, the largest cracks, where the gypsum crystallized very well, are only visible in the PZC and BFC samples, accounting for their worse behavior. Again the greater amount of calcium carbonate aggregate in S-specimens accounts for the greater source of calcium ions forming gypsum, which precipitation induces expansion.

To predict the life expectancy of concrete sewer pipes, even a phenomenological tool might be important for comparing the resistance and behavior of different concrete mixtures in cyclic contact with sulfuric acid and sulfates. Although it cannot predict the concrete's absolute life in quantitative terms, the results of our cyclic test enable the concrete's behavior and thinning to be

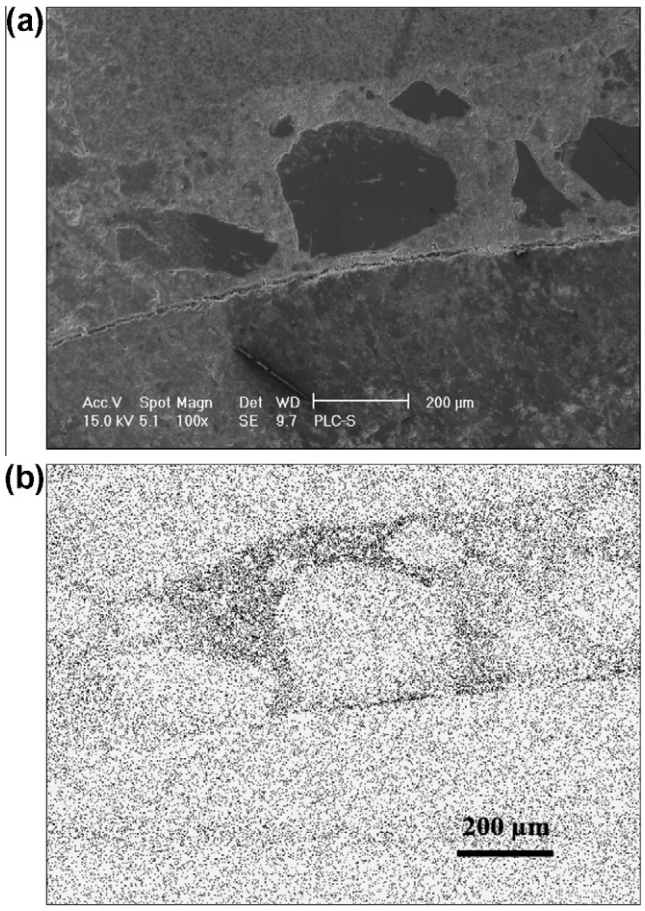

Fig. 10. SEM image (a) and X-ray maps for sulfur (dark) (b) on polished surface of PLC-S under cyclic sulfate/acid attack.

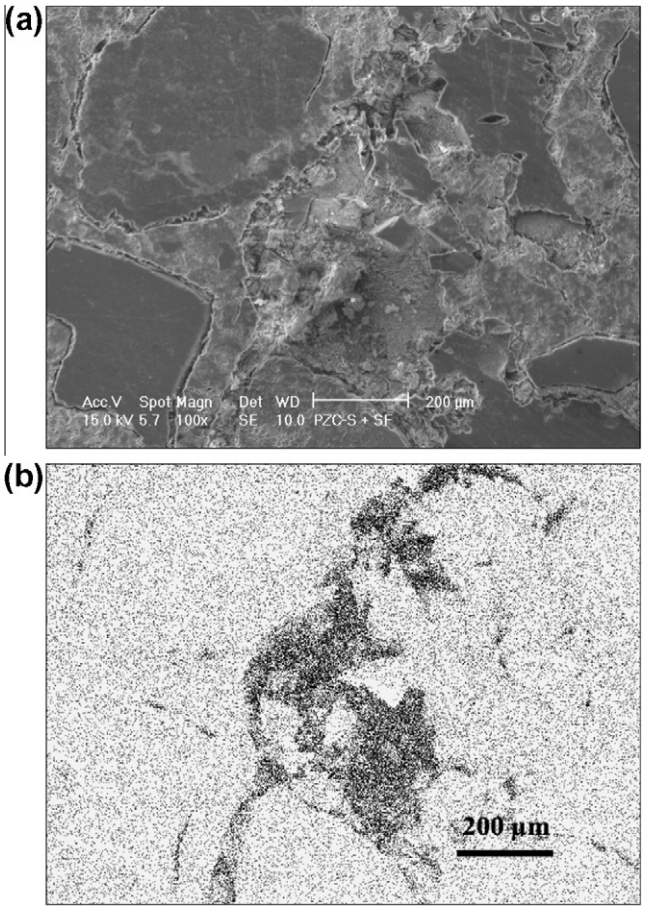

Fig. 11. SEM image (a) and X-ray maps for sulfur (dark) (b) on polished surface of PZC-S + SF under cyclic sulfate/acid attack.

assessed relatively quickly and reliably. The test might be further improved by taking the effect of temperature into account, studying the concretes at about 4–5 °C and with a minor concentration of sulfate ions, which favor the formation of ettringite and thaumasite.

5. Conclusions

We studied the deterioration of six different types of concrete either exposed continuously to a solution of several sulfates, or alternately to the mixed sulfate solution and to a solution of H_2SO_4 with a pH 2 for 6 h, once a month. The extent of the resulting damage was evaluated by measuring mass loss and expansion, in terms of strain. The results, charted for about 33,000 h, enabled the following conclusions to be drawn. The mixed sulfate solution caused more severe damage than is produced by sodium sulfate alone.

In general, the L-samples showed a shorter induction time before expansion than that of the S-samples. This is due mainly to the larger amount of calcium carbonate aggregate in the

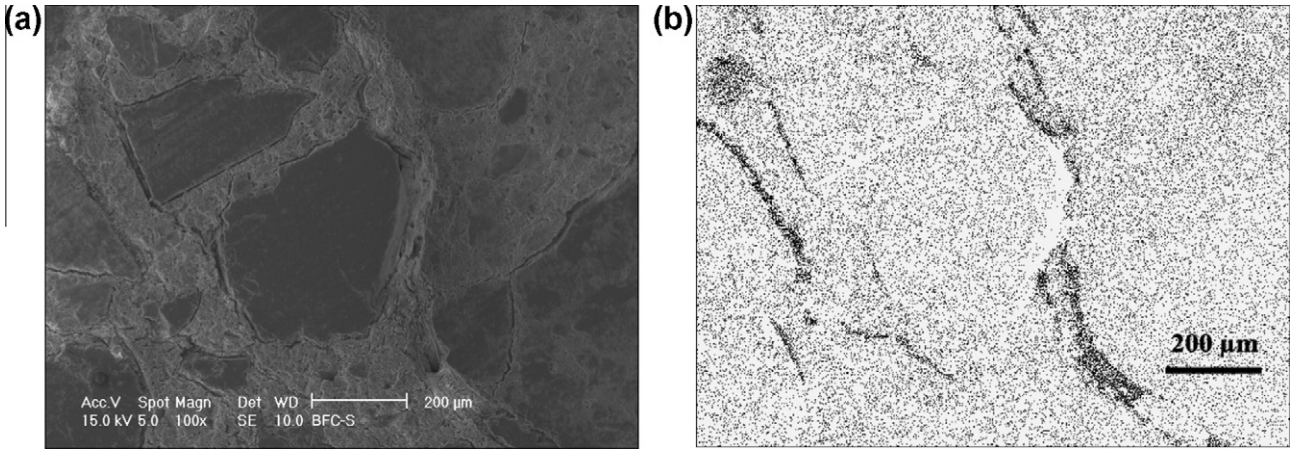

Fig. 12. SEM image (a) and X-ray maps for sulfur (dark) (b) on polished surface of BFC-S under cyclic sulfate/acid attack.

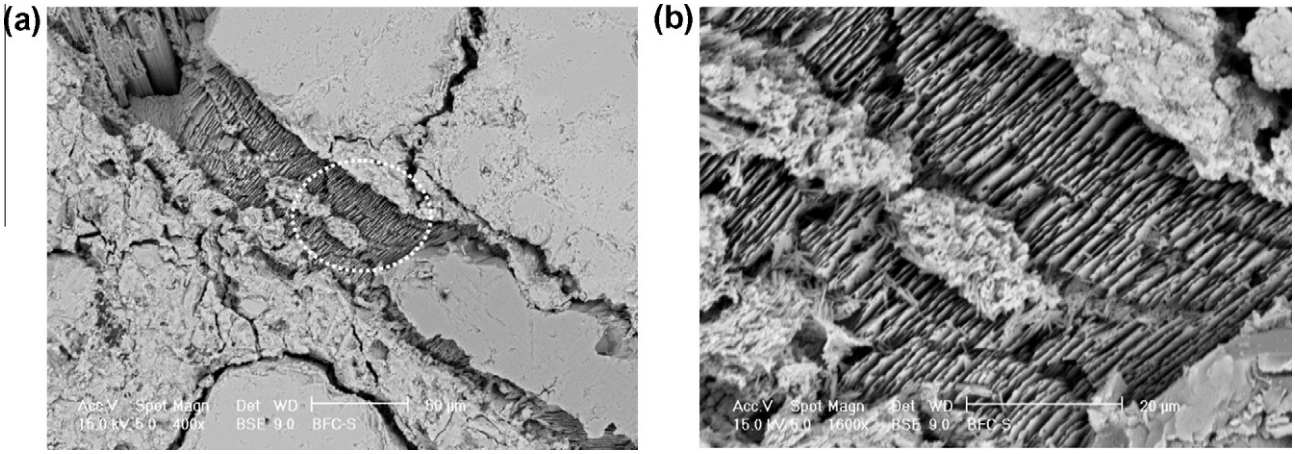

Fig. 13. SEM image of concrete BFC-S (a). The dashed red circle outlines the area magnified in (b), which contains layered crystals embedded in the cracks in the transition zone.

S-specimens, which is a source of calcium ions that form gypsum, the precipitation of which induces expansion.

The greatest expansion and most severe damage were surprisingly recorded for the BLF and PZC + SF samples, and took place in two stages. The cyclic exposure to mixed sulfates and sulfuric acid induced the greatest mass loss and expansion in the PZC + SF and BFC samples with natural aggregates. The effect of ammonium sulfate takes over from other species, reacting with portlandite and also with C–S–H especially in the transition zone around the aggregate and thus causing its detachment. A continuous web of cracks within the cement paste and through the aggregate particles was also apparent on SEM: according to the EDX analyses, the gypsum was only grown in the cracks and responsible for expansion and loss of aggregate. The larger amount of calcium carbonate in the aggregate of S-samples seems to be beneficial in order to reduce dissolution of C–S–H, but provides a source of calcium for gypsum formation and thus expansion.

The most interesting finding was that the concretes prepared with PLC fared better than the pozzolanic cement with silica fume or blast furnace cement. The formation of magnesium hydroxide accounts for PLC being the best choice for a concrete liable to attack by these different aggressive species, regardless of the aggregate used.

The method developed for this study proved very useful in comparing the resistance and behavior of different concrete mixtures in contact with a mixed sulfate with or without a cyclic exposure to sulfuric acid.

Acknowledgements

Publicemento ASSOBETON "Sezione Tubi" is gratefully acknowledged for funding the study. The authors would like to thank S. Cossalter and Eurobeton for their remarkable support in the research work. The authors are also grateful to C. Bonfanti, P. Bonora, U. Ursella, W. Vaona, F. Cona, E. D'Alessandro, M. Appoloni, M. Santolin, F. Zorzi and R. Zorzin for their interest and valuable help in collecting experimental data.

References

[1] Jahani F, Devinny J, Mansfeld F, Rosen IG, Sun Z, Wang C. Investigations of sulfuric acid corrosion of concrete. I: Modelling and chemical observations. Environ Eng 2001;127:572–9.
[2] Jahani F, Devinny J, Mansfeld F, Rosen IG, Sun Z, Wang C. Investigations of sulfuric acid corrosion of concrete. II: Electrochemical and visual observations. J Environ Eng 2001;127:580–4.
[3] Tulliani JM, Montanaro L, Negro A, Collepardi M. Sulfate attack of concrete building foundations induced by sewage waters. Cem Concr Res 2002;32:843–9.
[4] Torres SM, Sharp JH, Swamy RN, Lynsdale CJ, Huntley SA. Long term durability of Portland-limestone cement mortars exposed to magnesium sulfate attack. Cem Concr Res 2003;25:947–54.
[5] Vipulanandan C, Liu J. Glass-fiber mat-reinforced epoxy coating for concrete in sulfuric acid environment. Cem Concr Res 2002;32:205–10.
[6] Delagrave A, Pigeon M, Revertégat E. Influence of chloride ions and pH level on the durability of high performance cement pastes. Cem Concr Res 1994;24:1433–43.
[7] Parker CD. The corrosion of concrete. Aust J Exp Biol Med Sci 1945;23:91–8.
[8] Pavlík V, Uncík S. The rate of corrosion of hardened cement pastes and mortars with additive of silica fume in acids. Cem Concr Res 1997;27:1731–45.
[9] Scrivener KL, Cabiron J-L, Letourneux R. High-performance concretes from calcium aluminate cements. Cem Concr Res 1999;29:1215–23.
[10] Milde K, Sand W, Wolf W, Bock E. Thiobacilli of the corroded concrete wall of the Hamburg sewer. J Gen Microbiol 1988;123:1327–33.
[11] Fattuhi NI, Hughes BP. The performance of cement paste and concrete subjected to sulphuric acid attack. Cem Concr Res 1988;18:545–53.
[12] Attal A, Brigodiot M, Camacho P. Biological mechanisms of H_2S formation in sewer pipes. J Manem, Water Sci Technol 1992;26:907–14.
[13] Padival NA, Weiss JS, Arnold RG. Control of *Thiobacillus* by means of microbial competition: Implications for corrosion of concrete sewers. Water Environ Res 1995;67:201–5.
[14] Monteny J, De Belie N, Taerwe L. Resistance of different types of concrete mixtures to sulfuric acid. Mater Struct 2003;36:242–9.
[15] Beddoe RE, Dorner HW. Modelling acid attack on concrete: Part I. The essential mechanisms. Cem Concr Res 2005;35:2333–9.
[16] Hill J, Byars EA, Sharp JH, Lynsdale CJ, Cripps JC, Zhou Q. An experimental study of combined acid and sulfate attack of concrete. Cem Concr Compos 2003;25:997–1003.
[17] Durning TA, Hicks MC. Using microsilica to increase concrete's resistance to aggressive chemicals. Concr Int 1991;13:42–8.
[18] Girardi F, Vaona W, Di Maggio R. Resistance of different types of concretes to cyclic sulfuric acid and sodium sulfate attack. Cem Concr Res 2010;32:595–602.
[19] Santhanam M, Cohen MD, Olek J. Mechanism of sulfate attack: a fresh look. Part 1: Summary of experimental results. Cem Concr Res 2002;32:915–21.
[20] Santhanam M, Cohen MD, Olek J. Effects of gypsum formation on the performance of cement mortars during external sulfate attack. Cem Concr Res 2003;33:325–32.
[21] Santhanam M, Cohen MD, Olek J. Mechanism of sulfate attack: a fresh look. Part 2. Proposed mechanisms. Cem Concr Res 2003;33:341–6.
[22] Glasser FP, Marchand J, Samson E. Durability of concrete – Degradation phenomena involving detrimental chemical reactions. Cem Concr Res 2008;38:226–46.
[23] Mbessa M, Péra J. Durability of high-strength concrete in ammonium sulfate solution. Cem Concr Res 2001;31:1227–31.
[24] Miletić S, Ilić M,Ranogajec J,Marinovič-Neducin R,Djurić M. Portland ash cement degradation in ammonium-sulfate solution. Cem Concr Res 1998; 28:713–725.
[25] Higgins DD. Increased sulfate resistance of ggbs concrete in the presence of carbonate. Cem Concr Compos 2003;25:913–9.
[26] Haga K, Sutou S, Hironaga M, Tanaka S, Nagasaki S. Effects of porosity on leaching of Ca from hardened ordinary portland cement paste. Cem Concr Res 2005;35:1764–75.
[27] Mehta PK, Pirtz D, Polivka M. Properties of alite cements. Cem Concr Res 1979;9:439–50.

[28] Mehta PK. Materials Science of Concrete III. Am Ceram Soc, Westerville, OH; 1992.
[29] Santhanam M, Cohen MD, Olek J. Modeling the effects of solution temperature and concentration during sulfate attack on cement mortars. Cem Concr Res 2002;32:585–92.
[30] Tian B, Cohen MD. Does gypsum formation during sulfate attack on concrete lead to expansion? Cem Concr Res 2000;30:117–23.
[31] Bellmann F, Moeser B, Stark J. Influence of sulfate solution concentration on the formation of gypsum in sulfate resistance test specimen. Cem Concr Res 2006;36:358–63.